Latrunculin A and Its C-17-*O*-Carbamates Inhibit Prostate Tumor Cell Invasion and HIF-1 Activation in Breast Tumor Cells[⊥]

Khalid A. El Sayed,*[,†] Mohammad A. Khanfar,[†] Hassan M. Shallal,[†] A. Muralidharan,[†] Bhushan Awate,[†] Diaa T. A. Youssef,[‡] Yang Liu,[§] Yu-Dong Zhou,[§] Dale G. Nagle,[§] and Girish Shah[†]

Department of Basic Pharmaceutical Sciences, College of Pharmacy, University of Louisiana at Monroe, 700 University Avenue, Monroe, Louisiana 71209, Department of Pharmacognosy, Faculty of Pharmacy, Suez Canal University, Ismailia 41522, Egypt, and Department of Pharmacognosy, School of Pharmacy, University of Mississippi, University, Mississippi 38677-1848

Received October 21, 2007

The marine-derived macrolides latrunculins A (**1**) and B, from the Red Sea sponge *Negombata magnifica*, have been found to reversibly bind actin monomers, forming a 1:1 complex with G-actin and disrupting its polymerization. The microfilament protein actin is responsible for several essential functions within the cell such as cytokinesis and cell migration. One of the main binding pharmacophores of **1** to G-actin was identified as the C-17 lactol hydroxyl moiety that binds arginine 210 NH. Latrunculin A-17-*O*-carbamates **2**−**6** were prepared by reaction with the corresponding isocyanates. Latrunculin A (**1**) and carbamates **4**−**6** displayed potent anti-invasive activity against the human highly metastatic human prostate cancer PC-3M cells in a Matrigel assay at a concentration range of 50 nM to 1 μM. Latrunculin A (**1**, 500 nM) decreased the disaggregation and cell migration of PC-3M-CT+ spheroids by 3-fold. Carbamates **4** and **5** were 2.5- and 5-fold more active than **1**, respectively, in this assay with less actin binding affinity. Latrunculin A (**1**, IC_{50} 6.7 μM) and its 17-*O*-[*N*-(benzyl)carbamate (**6**, IC_{50} 29 μM) suppress hypoxia-induced HIF-1 activation in T47D breast tumor cells.

Latrunculins A (**1**) and B are macrolides reported by Kashman and co-workers from the Red Sea sponge *Negombata magnifica* Kelly Borges and Vacelet (Podospongiidae).[1] Latrunculins are reported to decrease intraocular pressure and increase outflow facility without corneal effects in monkeys.[2,3] Latrunculin B and analogues showed antiangiogenic, antimetastatic, and antimicrobial activities.[4] The most important biological effects of latrunculins are their abilities to disrupt microfilament organization and inhibit microfilament-mediated processes without affecting the organization of the microtubular system.[5] The latrunculins bind reversibly to the cytoskeleton actin monomers, forming 1:1 complexes with G-actin and disrupting polymerization.[5] Actin-active agents are attracting more attention in the field of cancer chemotherapy because microfilament and microtubule proteins form versatile dynamic polymers that can define cell polarity, organize cytoplasmic organelles, control cell shape and promote stable cell−cell and cell−matrix adhesions, and generate protrusive forces required for migration.[6–8] These functions usually fail and become abnormal in cancer cells.[6–8]

On the basis of X-ray crystallography, the binding site of **1** has been located between subdomains II and IV, in the vicinity of the ATP binding cleft of the protein target in the actin monomer.[9,10] The binding pharmacophores of **1** to G-actin were identified as follows: C-1 carbonyl oxygen through water to glutamate 214 carboxy, C-17 lactol hydroxyl to arginine 210 NH (major binding), C-17 pyran oxygen to tyrosine 69 hydroxy, thiazolidinone NH to aspartate 157 carboxy, and thiazolidinone C-20 carbonyl oxygen to threonine 186 hydroxy.[9,10] Only the thiazolidinone NH group acts as a hydrogen-bonding donor, while the rest of the binding functions act as hydrogen-bonding acceptors.[9,10]

Semisynthetic carbamoylation products of the C-17 lactol group in **1** were produced to study the pharmacological effects of the addition of hydrogen bond donors and acceptors at this key position. This study reports the anti-invasive and HIF-1 inhibitory activities of latrunculin A (**1**) and its semisynthetic analogues (**2**−**6**).

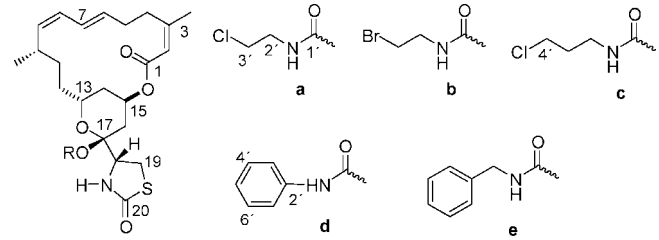

	R
1	H
2	**a**
3	**b**
4	**c**
5	**d**
6	**e**

Results and Discussion

Reflux of latrunculin A (**1**) in toluene with chloroethyl, bromoethyl, chloropropyl, benzyl, and phenyl isocyanates in the presence of catalytic amounts of triethylamine afforded the C-17-*O*-carbamates, **2**−**6**, respectively.

The HRMS analysis of compound **2** revealed the molecular formula, $C_{25}H_{35}ClN_2O_6S$, with $[M]^+$ and $[M + 2]^+$, 3:1, isotopic clusters characteristic for a monochlorinated compound. The downfield shift of the C-17 carbon and H-18 signals in **2** (+1.2 and 1.00 ppm, respectively) compared with that of the starting material **1** suggested possible carbamoylation at C-17, Table 1.[11] The ^1H and ^{13}C NMR data further supported this fact and were closely comparable to those of **1** except in the signals of an additional C-17-*O*-[*N*-(2-chloroethyl)carbamoyl] moiety (Tables 1 and 2).[11] The carbonyl carbon at δ_C 152.5 was assigned to C-1′. This was based on its ^3J-HMBC correlation with the methylene multiplet H_2-2′ (δ_H 3.61), which, in turn, showed $^1H-^1H$ COSY coupling with the H_2-3′ multiplet (δ_H 3.63).

Interpretation of the HRMS data of **3** suggested the molecular formula $C_{25}H_{35}BrN_2O_6S$, with characteristic isotopic clusters for a monobrominated compound. The ^1H and ^{13}C NMR data were

[⊥] Dedicated to Dr. G. Robert Pettit of Arizona State University for his pioneering work on bioactive natural products.

* To whom correspondence should be addressed. Tel: 318-342-1725. Fax: 318-342-1737. E-mail: elsayed@ulm.edu.

[†] University of Louisiana at Monroe.

[‡] Suez Canal University.

[§] University of Mississippi.

10.1021/np070587w CCC: $40.75
Published on Web 02/26/2008

Table 1. ^{13}C NMR Data of Compounds **2**−**6**[a]

	δ_C				
position	**2**	**3**	**4**	**5**	**6**
1	165.8, qC	165.5, qC	165.6, qC	165.5, qC	165.5, qC
2	117.4, CH	117.4, CH	117.4, CH	117.4, CH	117.4, CH
3	158.1, qC	158.2, qC	158.3, qC	158.2, qC	158.1, qC
4	32.6, CH_2	32.6, CH_2	32.6, CH_2	32.5, CH_2	32.5, CH_2
5	30.7, CH_2	30.6, CH_2	30.6, CH_2	30.5, CH_2	30.5, CH_2
6	131.8, CH	131.8, CH	132.0, CH	132.0, CH	131.9, CH
7	126.1, CH	126.0, CH	126.0, CH	125.9, CH	126.0, CH
8	127.8, CH	127.4, CH	127.4, CH	127.4, CH	127.4, CH
9	136.9, CH	136.4, CH	136.4, CH	136.4, CH	136.5, CH
10	29.2, CH	29.3, CH	29.2, CH	29.3, CH	29.3, CH
11	31.8, CH_2	31.8, CH_2	32.2, CH_2	31.8, CH_2	32.6, CH_2
12	31.5, CH_2	31.2, CH_2	31.5, CH_2	31.4, CH_2	31.5, CH_2
13	62.4, CH	62.3, CH	62.4, CH	62.4, CH	62.4, CH
14	35.0, CH_2	35.0, CH_2	35.0, CH_2	35.0, CH_2	35.0, CH_2
15	68.2, CH	68.2, CH	68.2, CH	68.2, CH	68.2, CH
16	35.2, CH_2	35.2, CH_2	35.2, CH_2	35.3, CH_2	35.2, CH_2
17	98.1, qC	98.1, qC	98.1, qC	98.1, qC	98.1, qC
18	62.9, CH	62.9, CH	62.9, CH	62.9, CH	62.9, CH
19	25.4, CH_2	25.5, CH_2	25.4, CH_2	25.4, CH_2	25.4, CH_2
20	176.2, qC	176.9, qC	177.0, qC	178.6, qC	177.2, qC
21	24.7, CH_3	25.0, CH_3	24.7, CH_3	24.6, CH_3	24.7, CH_3
22	21.9, CH_3	21.9, CH_3	21.9, CH_3	21.8, CH_3	21.8, CH_3
1′	152.5, qC	152.2, qC	152.4, qC	149.6, qC	151.2, qC
2′	42.2, CH_2	48.0, CH_2	37.7, CH_2	137.1, qC	41.5, CH_2
3′	43.2, CH_2	42.1, CH_2	31.8, CH_2	121.5, CH	141.5, qC
4′			42.3, CH_2	129.1, CH	127.0, CH
5′				124.5, CH	129.1, CH
6′				129.1, CH	126.5, CH
7′				121.5, CH	129.1, CH
8′					127.0, CH

[a] In $CDCl_3$, 100 MHz. Carbon multiplicities were determined by DEPT135° or APT experiments. qC = quaternary, CH = methine, CH_2 = methylene, CH_3 = methyl carbons.

similar to those of **2** with the replacement of chlorine at C-3′ by bromine (Tables 2). The methylene multiplet H_2-3′ (δ_H 3.69), which correlated with the methylene carbon at δ_C 42.1, was assigned on the basis of its $^1H-^1H$ COSY coupling with the H_2-2′ multiplet (δ_H 3.47, δ_C 48.0).

Analysis of the HRMS and ^1H and ^{13}C NMR data indicated **4** to be nearly identical in structure to **2**, except for the presence of an additional methylene carbon in the carbamate side chain (Tables 1 and 2). The broad methylene multiplet H_2-2′ (δ_H 3.47, δ_C 37.7) showed $^1H-^1H$ COSY coupling with the H_2-3′ multiplet (δ_H 1.42, δ_C 31.8). The latter protons showed a $^1H-^1H$ COSY coupling with the H_2-4′ triplet (δ_H 3.59, δ_C 42.3).

Interpretation of the HRMS and ^1H and ^{13}C NMR data of **5** indicated the presence of a 17-*O*-[*N*-(phenyl)carbamoyl] side chain (Tables 1 and 2). The broad doublet H_2-3′/7′ (δ_H 7.47, δ_C 121.5) showed COSY coupling with the H_2-4′/6′ double-doublet (δ_H 7.33, δ_C 129.1). The latter protons showed coupling in the COSY spectrum with the H-5′ multiplet (δ_H 7.15, δ_C 124.5).

Analysis of the HRMS and ^1H and ^{13}C NMR data indicated that the structure of **6** is closely similar to **5**, except that the phenyl group in **5** was replaced by a benzyl group in the carbamate side chain (Tables 1 and 2). The methylene doublet H_2-2′ (δ_H 4.39) showed a ^3J HMBC correlation with the carbonyl carbon at δ_C 153.5 (C-1′), confirming the 17-*O*-[*N*-(benzyl)carbamoyl] side chain.

Metastasis is the predominant cause of cancer mortality. The potential antimetastatic effects of compounds **1**−**6** against a human highly metastatic human prostate cancer PC-3M-CT+ cell line overexpressing calcitonin (CT) were evaluated using two in vitro models: linear invasion of cells through the Matrigel barrier and spheroid disaggregation.[13a–d] Latrunculin A (**1**) (100 nM) remarkably inhibited baseline and CT-stimulated invasion in the linear Matrigel assay (Figure 1). However, **1** was cytotoxic at doses higher than 500 nM (data not shown). There is evidence to suggest that cell migration and invasion involve multiple processes regulated by various signaling molecules.[14a–d] The actin cytoskeleton and its regulatory proteins are crucial for cell migration in most cells.[15a,b] During cell migration, the actin cytoskeleton is dynamically remodeled, and this reorganization produces the force necessary for cell migration.[15a,b] Since latrunculin A (**1**) attenuated invasiveness of PC-3M cells, its effect was examined on the actin cytoskeleton of PC-3M cells. PC-3M cells display an invasive phenotype, and they usually attach to the surface, exhibiting stretched actin fibers with long exon-type extensions (Figure 2A). Upon stimulation with 50 nM CT, the cells displayed rapid reorganization of the actin cytoskeleton, leading to visible changes in cell morphology within 10 min. The CT-stimulated cells demonstrated long actin-rich extensions resembling filopodia or microspikes or web-like actin-containing fibers linking these filopodium-like structures. However, the addition of latrunculin A (**1**) resulted in rapid changes in cell morphology and actin distribution as characterized by the remarkable shrinkage of actin stress fibers, possibly caused by the depolymerization disruption of actin (Figure 2B). Compound **1** also abolished CT-induced changes in the actin cytoskeleton. These results are consistent with the actions of latrunculin on PC-3M cell invasion (Figure 1) and suggest that anti-invasive actions of **1** are mediated through the disruption of actin cytoskeleton remodeling.

Spheroid disaggregation provides the measure of cell disaggregation as well as cell migration, and this model simulates the process of tissue disaggregation and invasion of cells in vivo.[13b,15c] This assay is based on disaggregation of cancer cell spheroids and radial migration of released cells on extracellular matrix (ECM).[13a–c,14d] Current evidence has shown that tumor cells from primary tumors in vivo are generally released in clumps, which attach to a favorable ECM and are later released gradually to migrate in all directions.[13a–13c,14d] Therefore, the spheroid disaggregation model is closer to in situ tumor metastasis than the linear Matrigel invasion assays. The results shown in Figure 3A demonstrate that latrunculin A (**1**, 500 nM) decreased disaggregation and cell migration of PC-3M-CT+ spheroids 3-fold. Figure 3B shows the antimetastatic

Table 2. ^{1}H NMR Data of Compounds **2**−**6**[a]

	δ_H				
position	**2**	**3**	**4**	**5**	**6**
2	5.65, brs	5.64, brs	5.64, brs	5.64, brs	5.65, brs
4	2.92, m 2.61, m	2.90, m 2.61, m	2.91, m 2.59, m	2.92, m 2.61, m	2.92, m 2.61, m
5	2.24, 2H, m	2.24, 2H, m	2.22, 2H, m	2.23, 2H, m	2.24, 2H, m
6	5.73, dt (14.8, 4.2)	5.74, dt (14.9, 4.2)	5.73, dt (15.4, 4.2)	5.72, dt (14.8, 4.2)	5.73, dt (14.8, 4.2)
7	6.41, dd (14.8, 10.0)	6.40, dd (14.9, 10.0)	6.41, dd (15.4, 10.0)	6.41, dd (14.8, 10.4)	6.41, dd (14.8, 10.0)
8	5.96, dd (10.5, 10.0)	5.97, dd (10.5, 10.0)	5.96, dd (10.5, 10.0)	5.97, dd (10.8, 10.4)	5.96, dd (10.5, 10.0)
9	4.99, dd (10.5, 10.5)	4.96, dd (10.6, 10.1)	4.99, dd (10.6, 10.6)	4.99, dd (10.7, 10.5)	4.99, dd (10.7, 10.5)
10	2.77, m	2.76, m	2.76, m	2.75, m	2.77, m
11	1.46, 2H, m	1.46, 2H, m	1.42, 2H, m	1.46, 2H, m	1.46, 2H, m
12	1.75, m 1.09, m	1.78, m 1.11, m	1.75, m 1.09, m	1.75, m 1.11, m	1.75, m 1.10, m
13	4.30, m	4.35, m	4.32, m	4.33, m	4.32, m
14	1.72, m 1.48, m	1.71, m 1.42, m	1.72, m 1.48, m	1.77, m 1.45, m	1.74, m 1.46, m
15	5.38, t (2.9)	5.37, t (2.8)	5.38, t (2.9)	5.38, t (2.8)	5.38, t (2.8)
16	2.00, dd (13.8, 3.5) 1.91, m	2.00, dd (13.8, 3.6) 1.92, m	1.98, m 1.88, m	2.08, dd (14.0, 3.6) 1.99, m	2.05, dd (14.0, 2.2) 1.99, m
18	4.85, brd (8.1)	4.85, d (8.0)	4.87, brd (8.1)	4.85, brd (8.1)	4.85, brd (8.1)
19	3.67, m 3.46, dd (10.9, 7.6)	3.67, m 3.46, dd (10.9, 7.6)	3.67, m 3.46, dd (10.9, 7.6)	3.63, m 3.52, m	3.67, m 3.46, m
21	1.89, 3H, brs	1.91, 3H, brs	1.90, 3H, brs	1.89, 3H, brs	1.89, 3H, brs
22	0.99, 3H, d (6.6)	0.95, 3H, d (6.6)	0.97, 3H, d (6.6)	0.98, 3H, d (6.6)	0.99, 3H, d (6.6)
2′	3.61, 2H, m	3.47, 2H, m	3.47, 2H, m	-	4.39, 2H, d (5.4)
3′	3.63, 2H, m	3.69, 2H, m	1.42, 2H, m	7.47, brd (8.1)	-
4′			3.59, 2H, t (6.2)	7.33, dd (8.1, 8.0)	7.27, brd (8.0)
5′				7.15, m	7.30, dd (8.0, 7.8)
6′				7.33, dd (8.1, 8.0)	7.32, dd (8.0, 7.8)
7′				7.47, brd (8.1)	7.30, dd (8.0, 7.8)
8′					7.27, brd (8.0)
NH	8.48, brs 4.11, s	8.49, t (5.2) 4.08, s	8.23, t, (5.8) 4.08, s	10.23, brs 4.15, s	9.28, brs 4.12, s

[a] In $CDCl_3$, 400 MHz. Coupling constants (J) are in Hz.

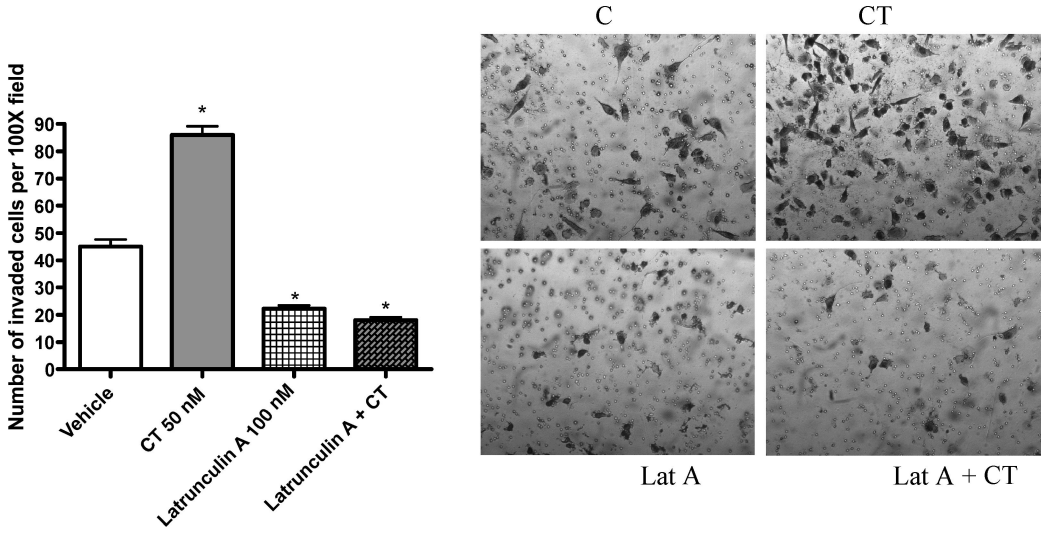

Figure 1. Anti-invasive activity of latrunculin A (**1**) against PC-3M-CT+ cells in a Matrigel assay.

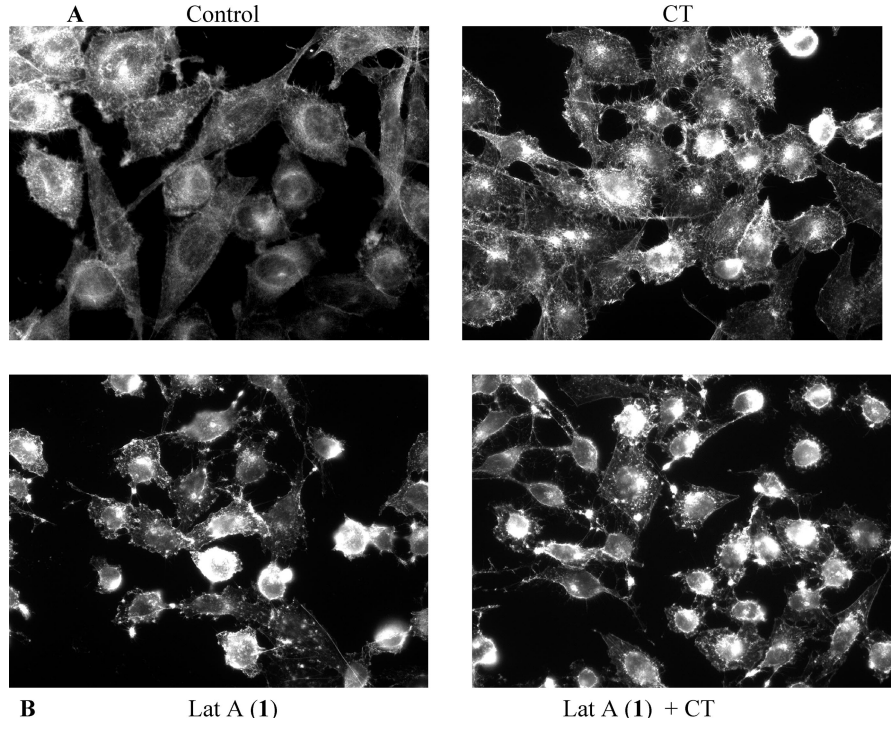

Figure 2. (A) PC3M cells displaying stretched actin fibers with long exon-type extensions (Control). CT (50 nM)-stimulated cells exhibit long actin-rich extensions resembling filopodia or web-like actin-containing fibers linking these filopodium-like structures (CT). (B) Addition of latrunculin A (**1**, 50 nM) resulted in rapid changes in cell morphology and actin distribution as characterized by the remarkable shrinkage of actin stress fibers (Lat A and Lat A + CT).

actions of latrunculin A (**1**) with analogues **4**−**6** at multiple doses. Analogues **4**−**6** also attenuated PC-3M-CT+ spheroid disaggregation/cell migration, and this response was dose-dependent in all three analogues tested. On the basis of the results shown in Figure 3B, analogue **5** was the most potent. Only a dose of 100 nM of analogue **5** was required to generate inhibition of PC-3M-CT+ spheroid disaggregation/cell migration to the extent of that produced by 500 nM of **1**. Compound **4** required 200 nM to produce the equivalent effect. Analogue **6** was equipotent to latrunculin A. Halogenated ethylcarbamates **2** and **3** were inactive, suggesting the significance of conjugation and extension of the carbamate side chain. The phenylcarbamate **5** was 2-fold more potent than benzylcarbamate **6**, suggesting the importance of optimum distance between the aromatic ring and the carbamate functionality for activity.

Relatively uncontrolled proliferation of cells within a tumor outstrips the capacity of existing vasculature to supply oxygen. This results in the formation of hypoxic regions within tumors. The occurrence of tumor hypoxia is associated with a poor prognosis in cancer patients.[16a] No drugs have been approved clinically to specifically target hypoxic tumor cells. The transcription factor hypoxia-inducible factor-1 (HIF-1) regulates hypoxia-induced gene expression in tumor cells that are subjected to hypoxic conditions.[16b] Disruption of HIF-1-mediated hypoxic adaptation/survival reduces tumor growth in animal models.[16c–i] HIF-1 inhibitors represent potential anticancer drug leads that may selectively target hypoxic tumor masses.[16j,k] The effects of **1**–**6** on hypoxia (1% O_2)-induced HIF-1 activation were examined using a T47D human breast carcinoma cell-based luciferase reporter assay[17] and compared to those observed on 1,10-phenanthroline-induced HIF-1 activation.

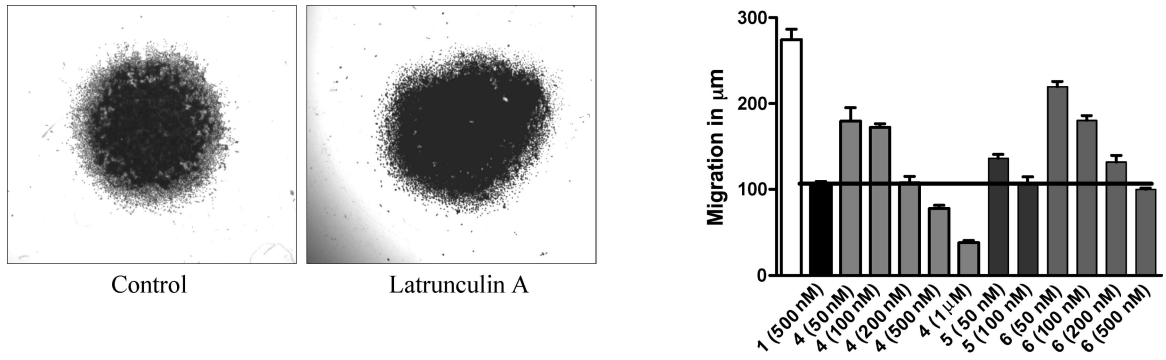

Figure 3. (A) Spheroid disaggregation of PC-3M-CT+ cells using 500 nM latrunculin A (**1**). (B) Spheroid disaggregation of PC-3M-CT+ cells comparison of different doses of carbamates **4**–**6** with the activity of latrunculin A (**1**).

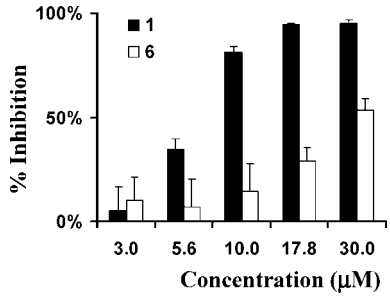

Figure 4. Effects of latrunculin A (**1**) and **6** on hypoxia-induced HIF-1 activation under hypoxic conditions in T47D breast carcinoma cells.

Compound **1** inhibited hypoxia-induced activation (IC_{50} 6.7 μM, Figure 4) and 1,10-phenanthroline-induced HIF-1 activation (IC_{50} 25 μM, data not shown). Compound **6** weakly inhibited hypoxia-induced HIF-1 activation (IC_{50} 29 μM). None of the other compounds (**2**−**5**) exerted greater than 50% inhibition of hypoxia-induced HIF-1 activation at the highest concentration tested (30 μM). The effects of **1**–**6** on the expression of luciferase from a control construct were examined in a T47D cell-based reporter assay and hypoxic cell viability/proliferation in a sulforhodamine B-based cell viability assay. None of the latrunculin analogues significantly inhibited the activity of a constitutively expressed pGL3 control reporter or significantly suppressed T47D cell viability under experimental conditions (less than 20% inhibition at the concentration of 30 μM). Therefore, latrunculin-based actin depolymerization disruptors appear to have the ability to selectively inhibit hypoxia-induced HIF-1 activity in tumor cells at concentrations below those evident for the inhibition of other critical cellular processes. The role of actin in HIF-1 signaling has never been documented. These results represent the first observation of the ability of actin inhibitors to inhibit HIF-1 activation at concentrations that also inhibit actin polymerization, and these findings may indicate that actin polymerization plays a vital role in HIF-1 signaling.

To further correlate the anti-invasive activity with the actin binding affinity, docking of **1**–**6** toward rabbit muscle α-actin was implemented using the SYBYL 7.3.4 and SurFlex-Dock programs. Docking results were expressed in three functions: total score, crash, and polar. The total score was expressed in $-\log(K_d)$ units to represent binding affinities. Crash is the degree of inappropriate penetration by the ligand into the protein and of interpenetration between ligand atoms that are separated by rotatable bonds. Crash scores close to 0 are favorable. Negative numbers indicate penetration. The polar score is the contribution of the polar non-hydrogen bonding interactions to the total score and may be useful for excluding docking results that involve no hydrogen bonds. The docking procedure was validated using the same conditions to dock

Table 3. Virtual Binding Affinity of Compounds **1**−**6** for Rabbit Muscle α-Actin Complex[a]

compound	score	crash	polar
1	6.24	−0.96	1.14
2	4.37	−2.52	0.00
3	4.60	−3.38	0.02
4	5.93	−2.80	0.01
5	6.12	−1.54	0.01
6	3.89	−2.97	2.46

[a] Using SYBYL 7.3.4, SurFlex-Dock 2.1.

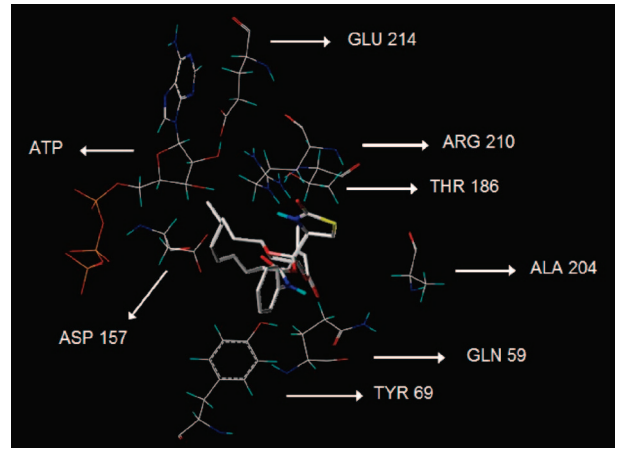

Figure 5. Detailed view of docked structure **5** with the corresponding rabbit muscle α-actin interacting amino acids.

latrunculin A (**1**) into the binding pocket of α-actin. The docking simulation resulted in a very close model to the crystallographic structure.[9,10] The docking data are summarized in Table 3.

The parent compound, latrunculin A (**1**), as well as the phenylcarbamate (**5**), showed the highest scores and molecular interaction, consistent with the observed anti-invasive activity (Table 3, Figure 5). The carbonyl oxygen of the carbamoyl moiety in **5** makes a strong H-bonding interaction with the guanidine amino group of arginine (ARG) 210 of actin (Figure 5). A similar interaction has been observed for carbamates **3** and **6**. Therefore, ARG 210 seems to play a central role in the binding of latrunculin A (**1**) and analogues within the actin monomers.[9,10] Although structure **6** showed anti-invasive activity, the scoring was the lowest among latrunculin A derivatives. Such deviation could be attributed to the activity of structure **6** on protein target(s) other than actin.

Experimental Section

General Experimental Procedures. Measurements of optical rotation were carried out on a Rudolph Research Analytical Autopol III polarimeter. IR spectra were recorded on a Varian 800 FT-IR

spectrophotometer. The ^1H and ^{13}C NMR spectra were recorded in $CDCl_3$, using TMS as an internal standard, on a JEOL Eclipse NMR spectrometer operating at 400 MHz for ^1H and 100 MHz for ^{13}C. The HREIMS experiments were conducted at the University of Michigan on a Micromass LCT spectrometer. TLC analysis was carried out on precoated silica gel 60 F_{254} 500 μm TLC plates, using the developing systems *n*-hexane−EtOAc (1:1) or $CHCl_3$−MeOH (9:1). For column chromatography, silica gel 60 (particle size 63–200 μm) or Bakerbond octadecyl (C_{18}), 40 μm, was used. For Sephadex LH-20 column chromatography, *n*-hexane−$CHCl_3$ (1:3), $CHCl_3$, and $CHCl_3$−MeOH (9:1) systems were used. For column chromatography, silica gel 70–230 mesh was used.

Biological Material. The sponge *Negombata magnifica* Kelly Borges and Vacelet (order Poecilosclerida, suborder Mycalina, family Podospongiidae) was collected as red, long, finger-like strips by scuba from the sand-covered bottom at −10 to −15 m at Hurghada, on the Egyptian Red Sea coast, in June 2003.[18,19] The sponge was identified by Mr. Tamer Helmy, Suez Canal University. A voucher specimen (03RS3) was deposited in the Department of Basic Pharmaceutical Sciences, College of Pharmacy, University of Louisiana at Monroe, Louisiana.

Extraction and Isolation. The frozen sponge (6 kg) was coarsely minced and extracted with $CHCl_3$ (5 × 1000 mL) at room temperature. The $CHCl_3$ extract was then concentrated under vacuum and subjected to liquid chromatography, as described elsewhere, to afford **1**, 1.2 g (0.0002%).[1,4,11]

Preparation of Carbamates 2–6. To solutions of 50 mg of **1** in toluene (2 mL) were added 59 μL of 2-chloroethyl isocyanate, 60 μL of 2-bromoethyl isocyanate, 60 μL of 3-chloropropyl isocyanate, 40 μL of phenyl isocyanate, or 36 μL of benzyl isocyanate, respectively, and separately mixed with 10 μL of Et_3N. Each solution was separately stirred at room temperature for 1 h (12 h for benzyl isocyanate only). Water (10 mL) was then added, and the product of each reaction mixture was extracted with EtOAc. Each EtOAc extract was dried over anhydrous Na_2SO_4 and concentrated under reduced pressure. Crude products were then purified by column chromatography on silica gel 60 using EtOAc−*n*-hexane, 1:9, to give compounds **2** (20.0 mg, 40% R_f 0.60, silica gel, $CHCl_3$−MeOH, 9.5:0.5) and **4** (13.2 mg, 26.4%, R_f 0.64), or EtOAc−*n*-hexane, 2:8, to give compounds **3** (13.3 mg, 26.6%, R_f 0.57) and **6** (19.4 mg, 38.8%, R_f 0.55), or $CHCl_3$−MeOH, 9.5:0.5, to afford compound **5** (13.6 mg, 27.2%, R_f 0.51).

17-*O*-[*N*-(2-Chloroethyl)carbamoyl]latrunculin A (2): colorless oil; $[\alpha]^{25}_D$ +48.8 (*c* 0.51, $CHCl_3$); IR ν_{max} (neat) 3564, 3331, 2953–2856, 1761, 1708, 1680, 1542, 1355, 1164 cm^{-1}; ^{13}C and ^1H NMR see Tables 1 and 2, respectively; HRESIMS *m/z* 549.1808 (calcd for $C_{25}H_{35}ClN_2O_6SNa$, 549.1802 $[M + Na]^+$).

17-*O*-[*N*-(2-Bromoethyl)carbamoyl]latrunculin A (3): colorless oil; $[\alpha]^{25}_D$ +30.0 (*c* 0.55, $CHCl_3$); IR ν_{max} (neat) 3563, 3327, 2995–2857, 1735, 1713, 1560, 1356, 1301, 1128 cm^{-1}; ^{13}C and ^1H NMR see Tables 1 and 2, respectively; HRESIMS *m/z* 593.1306 (calcd for $C_{25H35}BrN_2O_6SNa$, 593.1297 $[M + H]^+$).

17-*O*-[*N*-(3-Chloropropyl)carbamoyl]latrunculin A (4): colorless oil; $[\alpha]^{25}_D$ +50.3 (*c* 0.47, $CHCl_3$); IR ν_{max} (neat) 3564, 3335, 2953–2856, 1740, 1704, 1545, 1356, 1288, 1163 cm^{-1}; ^{13}C and ^1H NMR see Tables 1 and 2, respectively; HRESIMS *m/z* 563.1953 (calcd for $C_{26}H_{37}ClN_2O_6SNa$, 563.1959 $[M + H]^+$).

17-*O*-[*N*-(Phenyl)carbamoyl]latrunculin A (5): colorless oil; $[\alpha]^{25}_D$ +23.0 (*c* 0.14, $CHCl_3$);IR ν_{max} (neat) 3570, 3286, 2927–2853, 1710, 1601, 1680, 1554, 1446, 1296, 1160 cm^{-1}; ^{13}C and ^1H NMR see Tables 1 and 2, respectively; HRESIMS *m/z* 563.2200 (calcd for $C_{29}H_{36}N_2O_6SNa$, 563.2192 $[M + Na]^+$).

17-*O*-[*N*-(Benzyl)carbamoyl]latrunculin A (6): colorless oil; $[\alpha]^{25}_D$ +46.3 (*c* 0.55, $CHCl_3$); IR ν_{max} (neat) 3564, 3334, 2953–2857, 1730, 1703, 1680, 1542, 1455, 1357, 1282, 1166 cm^{-1}; ^{13}C and ^1H NMR see Tables 1 and 2, respectively; HRESIMS *m/z* 577.2360 (calcd for $C_{30}H_{38}N_2O_6SNa$, 577.2348 $[M + Na]^+$).

Invasion Assay. These experiments were conducted in 24-well, two-compartment, Matrigel invasion chambers (Becton Dickinson, Bedford, MA).[13a–d] The PC-3M-CT+ cells were grown exponentially under serum-starved conditions for 24 h [basal RPMI medium containing no serum or growth factors but containing 0.1% BSA, 10 mM HEPES, 4 mM L-glutamine, 100 IU mL^{-1} penicillin G, and 100 mg mL^{-1} streptomycin]. The cells were then harvested and seeded at a density of 25 × 10^3 cells per well in the upper insert of the Matrigel invasion chamber. The lower chamber received the chemoattractant medium, which consisted of 90% basal RPMI medium and 10% conditioned medium from the cultures of PC-3M-CT+ cells expressing constitutively active Gas protein. The incubation was carried out for 24 h, after which the Matrigel (along with noninvading cells) was scraped off with cotton swabs, and the outer side of the insert was fixed and stained using Diff Quick staining (Dade Behring Diagnostics, Aguada, Peurto Rico). The number of cells migrated on the outer bottom side of the insert was counted under the microscope in six or more randomly selected fields (magnification: 100×). Final results are expressed as mean ± SEM per 100× field. Each experiment was performed in triplicate, and the experiment was repeated twice.[13a–d]

Growth Correction. Since some cell lines can exhibit high proliferation rates, it is likely that the cells migrating during the early part of the 24 h incubation period could proliferate during the remaining period of incubation, leading to a slight overestimation of the final results. To correct this probability, the growth rate of PC-3M cells was determined under identical culture conditions. Twenty-five thousand cells were plated at hourly intervals in six-well dishes and cultured with/without CT (50 nM) for 1–24 h. Mean percent increase in the cell number was determined at the end of the incubation period by counting the net increase in the number of cells. The relative CT-induced increase of the pooled results of all time points was found to be 1.19 (vehicle control = 1). This correction was applied to the results of invasion assays.[13b,15d,e]

Spheroid Disaggregation Assay. Spheroids were prepared from single cell suspension of prostate cell lines as described before.[13b,d] In brief, 5 × 10^4/mL cells in RPMI 1640 serum-free medium were placed on 96-well low-attachment tissue culture plates. The plates were rocked on a gyrorotatory shaker in a CO_2 incubator at 37 °C for 2 days, at the end of which the spheroids measuring 150–300 μm in diameter (~4 × 10^4 cells/spheroid) were formed. A single spheroid was then placed in the center of each well of an extracellular matrix (ECM)-coated 24-well microplate in 200 mL of serum-free medium. From previous studies, it was determined that 1 h is an appropriate time for spheroids to begin adhering to an ECM. Thus $t = 0$ was set as 1 h from initial plating, so that if the plate was not disturbed, the spheroids would not move from their location at the time of plating. Spheroids were photographed digitally at $t = 0$, cultured at 37 °C for 48 h, and then rephotographed. The spheroids were then fixed, stained with Diff-Quik (Dade Behring, Newark, DE), and examined under light microscopy. The diameter of the area covered with cells migrated from the spheroids was measured in a microscope calibrated with a stage and ocular micrometer. The radial distance of migration was calculated after subtraction of the mean initial spheroidal diameter at $t = 0$. Values shown represent the average percent increase in surface area of spheroids.

Cell Proliferation/Viability Assay. Human breast carcinoma T47D cells were grown in DMEM/F12 medium with L-glutamine (Mediatech) supplemented with 10% (v/v) fetal calf serum (FCS, Hyclone), 50 units mL^{-1} penicillin G (Na salt), and 50 μg mL^{-1} streptomycin sulfate (referred to as "Pen/Strep") (Invitrogen) in a humidified atmosphere (5% CO_2/95% air) at 37 °C. Exponentially grown cells were plated at a density of 30 000 cells per well into 96-well tissue culture plates (Corning) in a volume of 100 μL of DMEM/F12 medium with 10% FCS and Pen/Strep. The cells were incubated at 37 °C overnight.[17,20] Test compounds were diluted in DMEM/F12 medium with Pen/Strep and added in a volume of 100 μL per well. Following a 30 min incubation, the compound treatment continued for another 16 h (or 48 h) at 37 °C under hypoxic (5% CO_2/1% O_2/94% N_2) or normoxic (5% CO_2/95% air) conditions. Cell proliferation/viability (performed in triplicate) was determined as previously described.[17,20] The absorbance at 515 nm was measured on a BioTek Synergy HT microplate reader with correction wavelength at 690 nm. The data were normalized to the untreated control. The following formula was used to calculate % inhibition of cell proliferation/viability: % inhibition = 1 − OD_{515}(treated)/OD_{515}(control).

Cell-Based Reporter Assay for HIF-1 Activity. The transfection, compound treatment, exposure to hypoxic conditions (5% CO_2/1% O_2/94% N_2), normoxic conditions (5% CO_2/95% air), and a hypoxia mimetic (10 μM 1,10-phenanthroline), and luciferase activity determination were performed as previously described.[20] Emetine was used as a positive control (IC_{50} 0.11 μM).

Molecular Modeling. Docking and scoring modeling studies were

performed using SYBYL 7.3.4 (Tripos Discovery Informatics, St. Louis, MO) installed on a Dell desktop workstation equipped with a 1.86 GHz Intel Xeon processor and the Red Hat Enterprise Linux (version 4) operating system. The 3D coordinates of rabbit muscle α-actin complex with latrunculin A (**1**) were retrieved from the Protein Data Bank (PDB code: 1esv). The selected structure is of the best 3D resolution (2.0 Å). The protein structure was utilized in subsequent docking experiments without energy minimization. Explicit water molecules were removed from the structure. Chemical structures of **1**−**6** were drawn in SYBYL 7.3.4 and assigned Gasteiger partial charges and energy minimized using Energy Force Field. Docking simulations of structures **1**−**6** were carried out using SurFlex-Dock (version 2.1). SurFlex-Dock identifies the active site of the protein and constructs a docking target (protomol) to which molecules match. Protmol was generated by the ligand-based method, setting the Threshold and Bloat parameters as default value (0.5 and 0.0, respectively).

Acknowledgment. This investigation was made possible through the support of NIH grant number P20RR16456 from the BRIN Program of the National Center for Research Resources, grant R01CA96534 (G.V.S.), and grant CA98787 (D.G.N., Y.-D.Z.). Its contents are solely the responsibility of the authors and do not necessarily represent the official views of NIH. Louisiana Board of Regents grant LEQSF(2007-08)-ENH-TR-80 is acknowledged for the support of the purchase of the NMR probe.

References and Notes

(1) Kashman, Y.; Groweiss, A.; Shmueli, U. *Tetrahedron Lett.* **1980**, *21*, 3629–3632.
(2) Okka, M.; Tian, B.; Kaufman, P. L. *Arch. Ophthalmol.* **2004**, *122*, 1482–1488.
(3) Kaufman, P. L.; Geiger, B. *U.S. Patent* 772,412, 2002.
(4) El Sayed, K. A.; Youssef, D. T. A.; Marchetti, D. *J. Nat. Prod.* **2006**, *69*, 219–223.
(5) Spector, I.; Shochet, N. R.; Blasberger, D.; Kashman, Y. *Cell Motil. Cytoskel.* **1989**, *13*, 127–144.
(6) Newman, D. J.; Cragg, G. M. *J. Nat. Prod.* **2004**, *67*, 1216–1238.
(7) Nakaseko, Y.; Yanagida, M. *Nature* **2001**, *412*, 291–292.
(8) Gachet, Y.; Tournier, S.; Millar, J. B.; Hyams, J. S. *Nature* **2001**, *412*, 352–355.
(9) Yarmola, E. G.; Somasundaram, T.; Boring, T. A.; Spector, I.; Bubb, M. R. *J. Biol. Chem.* **2000**, *275*, 28120–28127.
(10) Morton, W. M.; Ayscough, K. R.; McLaughlin, P. J. *Nat. Cell Biol.* **2000**, *2*, 376–378.
(11) Groweiss, A.; Shmueli, U.; Kashman, Y. *J. Org. Chem.* **1983**, *48*, 3512–3516.
(12) Blasberger, D.; Carmely, S.; Cojocaru, M.; Spector, I.; Shochet, N. R.; Kashman, Y. *Liebigs Ann. Chem.* **1989**, *12*, 1171–1188.
(13) (a) Shah, G. V.; Noble, M. J.; Austenfeld, M.; Weigel, J.; Deftos, L. J.; Mebust, W. K.; Winston, K. *Prostate* **1992**, *21*, 87–97. (b) Thomas, S.; Chigurupati, S.; Anbalagan, M.; Shah, G. *Mol. Endocrinol.* **2006**, *20*, 1894–1911. (c) Chien, J.; Ren, Y.; Wang, Y. Q.; Bordelon, W.; Thompson, E.; Davis, R.; Rayford, W.; Shah, G. *Mol. Cell. Endocrinol.* **2001**, *181*, 69–79. (d) Thomas, S.; Chiriva-Internati, M.; Shah, G. V. *Clin. Exp. Metastasis* **2007**, *24*, 363–377.
(14) (a) Cooper, C. R.; Chay, C. H.; Pienta, K. J. *Neoplasia* **2002**, *4*, 191–194. (b) Ghosh, P. M.; Ghosh-Choudhury, N.; Moyer, M. L.; Mott, G. E.; Thomas, C. A.; Foster, B. A.; Greenberg, N. M.; Kreisberg, J. I. *Oncogene* **1999**, *18*, 4120–4130. (c) Chen, Y.; Wang, Y.; Yu, H.; Wang, F.; Xu, W. *Exp. Biol. Med.* **2005**, *230*, 731–741. (d) Alroy, I.; Yarden, Y. *FEBS Lett.* **1997**, *410*, 83–86. (e) Hoevel, T.; Macek, R.; Swisshelm, K.; Kubbies, M. *Int. J. Cancer* **2004**, *108*, 374–383.
(15) (a) Byers, H. R.; Etoh, T.; Doherty, J. R.; Sober, A. J.; Mihm, M. C. *Am. J. Pathol.* **1991**, *139*, 423–435. (b) Hotulainen, P.; Paunola, E.; Vartiainen, M. K.; Lappalainen, P. *Mol. Biol. Cell* **2005**, *16*, 649–664. (c) Cascone, I.; Giraudo, E.; Caccavari, F.; Napione, L.; Bertotti, E.; Collard, J. G.; Serini, G.; Bussolino, F. *J. Biol. Chem.* **2003**, *278*, 50702–50713. (d) Yoshioka, K.; Nakamori, S.; Itoh, K. *Cancer Res.* **1999**, *59*, 2004–2010. (e) Gondi, C. S.; Lakka, S. S.; Yanamandra, N.; Olivero, W. C.; Dinh, D. H.; Gujrati, M.; Tung, C. H.; Weissleder, R.; Rao, J. S. *Cancer Res.* **2004**, *64*, 4069–4077.
(16) (a) Tatum, J. L.; Kelloff, G. J.; Gillies, R. J.; Arbeit, J. M.; Brown, J. M.; Chao, K. S.; Chapman, J. D.; Eckelman, W. C.; Fyles, A. W.; Giaccia, A. J.; Hill, R. P.; Koch, C. J.; Krishna, M. C.; Krohn, K. A.; Lewis, J. S.; Mason, R. P.; Melillo, G.; Padhani, A. R.; Powis, G.; Rajendran, J. G.; Reba, R.; Robinson, S. P.; Semenza, G. L.; Swartz, H. M.; Vaupel, P.; Yang, D.; Croft, B.; Hoffman, J.; Liu, G.; Stone, H.; Sullivan, D. *Int. J. Radiat. Biol.* **2006**, *82*, 699–757. (b) Semenza, G. L. *Nat. Rev. Cancer* **2003**, *3*, 721–732. (c) Maxwell, P. H.; Dachs, G. U.; Gleadle, J. M.; Nicholls, L. G.; Harris, A. L.; Stratford, I. J.; Hankinson, O.; Pugh, C. W.; Ratcliffe, P. J. *Proc. Natl. Acad. Sci. U.S.A.* **1997**, *94*, 8104–8109. (d) Ryan, H. E.; Lo, J.; Johnson, R. S. *EMBO J.* **1998**, *17*, 3005–3015. (e) Ryan, H. E.; Poloni, M.; McNulty, W.; Elson, D.; Gassmann, M.; Arbeit, J. M.; Johnson, R. S. *Cancer Res.* **2000**, *60*, 4010–4015. (f) Kung, A. L.; Wang, S.; Klco, J. M.; Kaelin, W. G.; Livingston, D. M. *Nat. Med.* **2000**, *6*, 1335–1340. (g) Kung, A. L.; Zabludoff, S. D.; France, D. S.; Freedman, S. J.; Tanner, E. A.; Vieira, A.; Cornell-Kennon, S.; Lee, J.; Wang, B.; Wang, J.; Memmert, K.; Naegeli, H. U.; Petersen, F.; Eck, M. J.; Bair, K. W.; Wood, A. W.; Livingston, D. M. *Cancer Cell* **2004**, *6*, 33–43. (h) Unruh, A.; Ressel, A.; Mohamed, H. G.; Johnson, R. S.; Nadrowitz, R.; Richter, E.; Katschinski, D. M.; Wenger, R. H. *Oncogene* **2003**, *22*, 3213–3220. (i) Moeller, B. J.; Dreher, M. R.; Rabbani, Z. N.; Schroeder, T.; Cao, Y.; Li, C. Y.; Dewhirst, M. W. *Cancer Cell* **2005**, *8*, 99–110. (j) Semenza, G. L. *Expert Opin. Ther. Targets* **2006**, *10*, 267–280. (k) Melillo, G. *Cancer Metastasis Rev.* **2007**, *16*, 341–352.
(17) Dai, J.; Liu, Y.; Zhou, Y.-D.; Nagle, D. G. *J. Nat. Prod.* **2007**, *70*, 130–133.
(18) Kelly-Borges, M.; Vacelet, J. *Mem. Queensl. Mus.* **1995**, *38*, 477–503.
(19) Antunes, E. M.; Copp, B. R.; Davies-Coleman, M. T.; Samaai, T. *Nat. Prod. Rep.* **2005**, *22*, 62–72.
(20) Hodges, T. W.; Hossain, F. C.; Kim, Y.-P.; Zhou, Y.-D.; Nagle, D. G. *J. Nat. Prod.* **2004**, *67*, 767–771.

NP070587W